



## 28 **ABSTRACT**

29 This study evaluated the effects of producing warm mix asphalt (WMA) at lower temperatures, compared to  
30 conventional hot mix asphalt (HMA), on energy consumption and asphalt mixture performance at both material and  
31 pavement levels. Two field projects were conducted in Alabama. The first evaluated two chemical WMA additives,  
32 while the second assessed further temperature reductions using one of the WMA additives with a different mix  
33 design. Burner fuel usage was monitored during production to quantify energy savings. Laboratory testing using the  
34 Asphalt Mixture Performance Tester (AMPT) included dynamic modulus ( $|E^*|$ ), cyclic fatigue, and stress sweep  
35 rutting (SSR) tests. The FlexMAT™ v2.2 program was used to analyze mechanistic test results, and pavement  
36 performance—specifically, fatigue cracking and rutting—was evaluated using FlexPAVE™ v2.2 under  
37 representative traffic and climate conditions. In Experiment 1, limited temperature reductions resulted in no  
38 significant difference in burner fuel consumption among mixtures. In Experiment 2, production temperature  
39 reductions of 22°C (40°F) and 36°C (65°F) yielded burner fuel savings of approximately 8% and 19%, respectively.  
40 Across both experiments, WMA mixtures demonstrated lower mixture Glover–Rowe ( $G-Rm$ ) values, indicating  
41 improved non-load-related cracking resistance, while cyclic fatigue indices ( $D^R$  and  $S_{app}$ ) were similar to those of  
42 HMA control mixtures. However, WMA mixtures exhibited increased rutting susceptibility and higher Rutting  
43 Strain Index (RSI) values, especially at the lowest production temperature. FlexPAVE™ v2.2 modeling predicted  
44 slightly higher fatigue damage and rutting in WMA mixtures compared with HMA. Overall, the findings suggest  
45 that WMA technologies can substantially reduce burner fuel use while maintaining acceptable pavement  
46 performance, provided mix design adjustments are made to control rutting at lower production temperatures.

47

## 48 **PRACTICAL APPLICATIONS**

49 The findings of this study offer practical insights for highway agencies, contractors, and pavement engineers seeking  
50 to reduce energy consumption and environmental impacts from asphalt mixture production while maintaining  
51 satisfactory pavement performance. The implementation of WMA technologies can significantly lower burner fuel  
52 consumption, thereby reducing operational costs and emissions at production facilities. Additionally, WMA  
53 mixtures demonstrated improved cracking resistance, suggesting potential long-term durability benefits. However,

54 when production temperatures are significantly reduced, adjustments to the mixture design may be necessary to  
55 mitigate the increased risk of rutting susceptibility.

56

## 57 **AUTHOR KEYWORDS**

58 Warm Mix Asphalt (WMA); Burner Fuel Consumption; Cracking Resistance; Rutting Susceptibility; Dynamic  
59 Modulus, Cyclic Fatigue, Performance Modeling; Emissions.

60

## 61 **INTRODUCTION**

62 The asphalt paving industry continues to advance through the adoption of innovative technologies aimed at  
63 improving production efficiency, optimizing material usage, improving sustainability, and extending pavement  
64 service life. Among these innovations, warm mix asphalt (WMA), recycling agents, advancements in pavement  
65 recycling, and balanced mix design (BMD) approaches have demonstrated considerable potential to improve  
66 pavement performance and resource efficiency (Epps 2019; Sadeghi and Sabouri 2025).

67 WMA refers to asphalt mixtures produced and placed at significantly lower temperatures than conventional hot mix  
68 asphalt (HMA). These temperature reductions are achieved using technologies in three general categories: foaming  
69 technologies, organic (wax-based) additives, and chemical additives (Cheraghian et al. 2020). Water-based foaming  
70 increases binder volume and surface area, thereby reducing viscosity and improving workability. Wax-based  
71 additives also reduce binder viscosity, thereby improving workability. Surfactant-based chemical additives lower  
72 interfacial friction between the binder and aggregate, facilitating easier mixing and compaction.

73 Beyond improved compactability, WMA technologies offer several additional advantages, including reduced  
74 emissions, longer haul distances, extended paving seasons, and the ability to incorporate more recycled materials  
75 (Capitão et al. 2012; Rubio et al. 2012; Sukhija et al. 2022; Zaremotekhasas et al. 2022). One of the primary  
76 motivations for adopting WMA is the opportunity to reduce energy consumption and greenhouse gas (GHG)  
77 emissions during production (Rubio et al. 2012; Sukhija et al. 2022). Reported energy savings vary depending on  
78 additive type, plant configuration, fuel source, aggregate moisture content, and production temperature. For

79 example, Sukhija et al. (2022) reported that WMA production reduced heat energy demand by 3–12%, with the  
80 highest reductions achieved using organic additives (4–12%), followed by chemical additives (3–10%) and foamed  
81 technologies (up to 9%). Almeida-Costa and Benta (2016) reported manufacturing energy reductions of  
82 approximately 18.4% and 8.6% for temperature drops of 46°C and 20°C, respectively, noting that fuel savings could  
83 offset additive costs. Similarly, West et al. (2014) documented an average burner fuel savings of 22.1% across six  
84 asphalt plants, corresponding to an average temperature reduction of 26.7°C. A multi-state study found that lowering  
85 the production temperature by approximately 30°C with a chemical WMA additive reduced burner fuel consumption  
86 by about 20% (NAPA 2024).

87 These energy savings translate directly to environmental benefits. For example, a study across five states observed  
88 an average 22.3% reduction in stack CO<sub>2</sub> emissions when WMA mixtures were produced 30°C below HMA  
89 temperatures (NAPA 2024). Croteau and Tessier (2008) estimated that each ton of WMA produced results in 4.1 to  
90 5.5 kg less CO<sub>2</sub> equivalent emissions. According to the National Asphalt Pavement Association (NAPA), the use of  
91 WMA in the U.S. in 2022 led to a reduction of approximately 0.18 million metric tons of CO<sub>2</sub> equivalent—  
92 comparable to the annual emissions of 40,000 passenger vehicles (Williams et al. 2024).

93 In terms of performance, extensive research over the past two decades has examined the material and structural  
94 behavior of WMA mixtures. Lower production temperatures reduce oxidative aging, resulting in more flexible and  
95 less brittle mixtures (Dao et al. 2022; Yin et al. 2023). A field study revealed that chemical WMA exhibited lower  
96 stiffness than the corresponding HMA, and this difference persisted over time (Spadoni et al. 2022). Laboratory  
97 evaluations have also confirmed improved intermediate-temperature cracking resistance for WMA mixtures, as  
98 shown by higher Indirect Tensile Asphalt Cracking Test (IDEAL-CT) results (Sadeghi et al. (2025) and improved  
99 flexibility index and semi-circular bending performance (Rahman et al. (2022). While the extent of improvement  
100 depends on the additive type and test conditions, WMA mixtures generally demonstrate enhanced cracking  
101 performance (Padula et al. 2019).

102 Regarding rutting performance, most studies report that the slightly softer binders and lower aging associated with  
103 WMA production do not significantly compromise resistance to permanent deformation. For example, Bairgi et al.  
104 (2020) found that three WMA mixtures using foamed, Evotherm, and Cecabase additives showed slightly higher  
105 laboratory and field rutting than the control HMA; however, all sections exhibited acceptable field performance,

106 with only 2–3 mm of rut depth after five years. Similar findings have been reported in other studies (Bairgi et al.  
107 2018; Wen et al. 2016). Long-term field trials have confirmed that WMA pavements generally perform comparably  
108 to HMA pavements after several years of service (McCarthy and Daniel 2018). Because the Superpave mix design  
109 system has largely eliminated rutting problems (West et al. 2018), current WMA research focuses on improving  
110 cracking resistance and lowering production temperatures while maintaining rutting within acceptable limits. A  
111 previous study reported mostly comparable laboratory cracking and rutting performance properties for plant-mixed  
112 WMA mixtures, while more significant differences were noted between lab-mixed samples (Sadeghi et al. 2025).  
113 In addition to laboratory testing, pavement modeling tools such as the Federal Highway Administration's  
114 FlexPAVE™ have been used to predict long-term pavement performance. FlexPAVE™ integrates mixture  
115 properties, traffic loading, and climate data to simulate viscoelastic pavement responses (FHWA 2025) and aging  
116 effects through a calibrated model developed under NCHRP Project 09-54 (Kim et al. 2021). Studies have shown  
117 that FlexPAVE™ can predict rutting and cracking trends consistent with field performance (Ghanbari et al. 2022;  
118 Wang et al. 2016).

119 Despite the promising outcomes, uncertainties persist regarding the long-term performance of WMA, particularly  
120 under harsh environmental or heavy traffic conditions. For example, WMA test sections in Louisiana exhibited  
121 lower fatigue cracking than HMA after 5–8 years (Akontuna et al. 2022). While some chemical additives enhance  
122 moisture resistance, others may increase moisture sensitivity if reduced production temperatures limit aggregate  
123 drying (Fakhri et al. 2013) (Garcia Cucalon et al. 2017; Zaumanis 2014). Consequently, many agencies and  
124 contractors still use WMA primarily as a compaction aid rather than significantly lowering production temperatures.  
125 Continued long-term field evaluations, along with advanced mechanistic modeling, are crucial for validating WMA  
126 durability and supporting broader implementation under diverse climatic and traffic conditions.

## 127 128 **Objectives and Scope**

129 The primary objective of this study was to evaluate the impact of reducing asphalt production temperatures with  
130 WMA additives on burner fuel consumption, mixture fundamental properties, and predicted pavement performance.  
131 Two field demonstration projects were conducted, each including two WMA mixtures and one control HMA.

132 In the first project, two chemical WMA additives were evaluated against the control HMA. One of the WMA  
133 additives was used in the second project, which focused on evaluating the effects of further reducing the production  
134 temperature.

135 Burner fuel consumption was recorded during plant production to quantify energy savings. Fundamental mixture  
136 properties were evaluated using the Asphalt Mixture Performance Tester (AMPT), which included dynamic  
137 modulus, cyclic fatigue, and Stress Sweep Rutting (SSR) tests. The test results were analyzed using the FlexMAT™  
138 program to assess material performance properties, while the FlexPAVE™ modeling tool was employed to predict  
139 pavement performance, including percent damage and rutting. Through this integrated experimental and modeling  
140 approach, the study provides a comprehensive assessment of the energy consumption and performance associated  
141 with reducing production temperatures using WMA additives.

142

## 143 **METHODOLOGY**

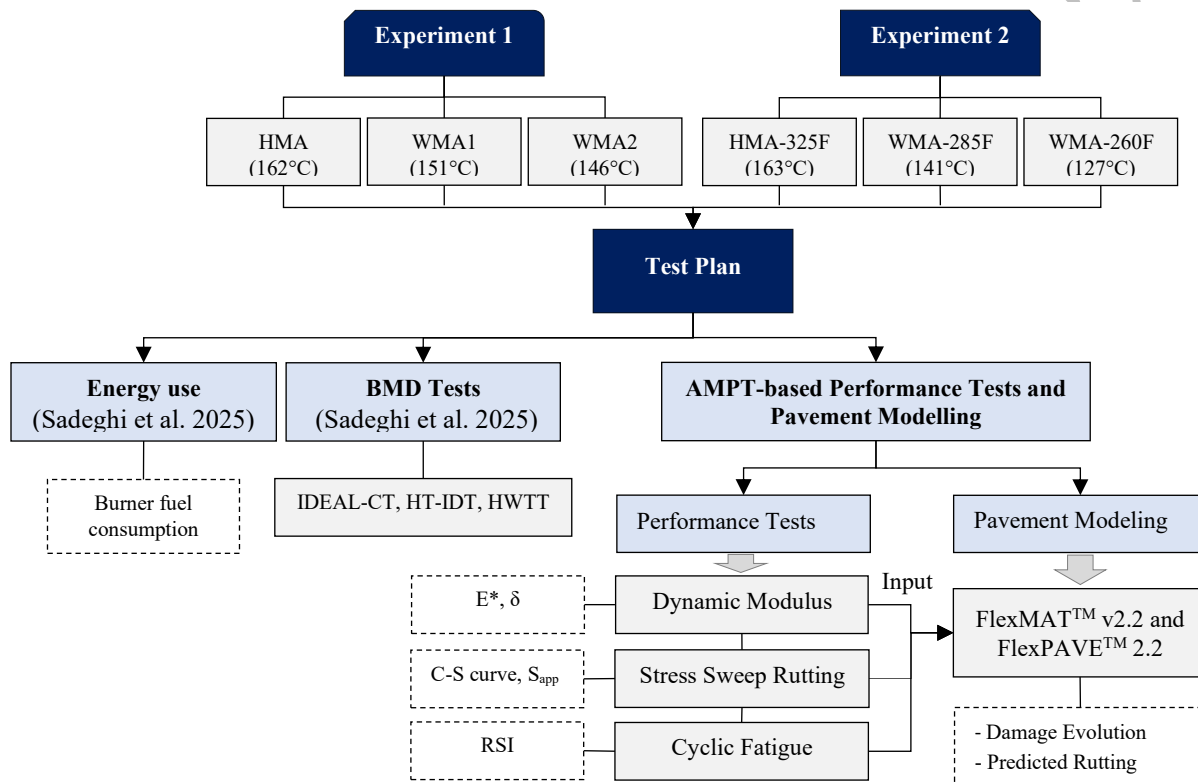
### 144 **Experimental Plan**

145 This study was structured in three main phases:

- 146 1. Quantifying energy savings associated with producing WMA at reduced temperatures
- 147 2. Evaluating mixture performance using IDEAL-CT, Hamburg Wheel-Tracking Test (HWTT), and High-  
148 Temperature Indirect Tensile Test (HT-IDT)
- 149 3. Assessing the fundamental properties using the AMPT tests and predicting the pavement performance of  
150 WMA mixtures compared to conventional HMA.

151 The findings from Phases 1 and 2 have been previously published (Sadeghi et al. 2025). This paper will concentrate  
152 on the results of Phase 3, with a brief overview of Phase 1 included to emphasize the environmental significance of  
153 the performance outcomes. This context will facilitate an understanding of the mechanistic testing and modeling  
154 conducted during Phase 3. It is also essential to note that while direct comparisons were made within each  
155 experiment, cross-experiment comparisons were not conducted due to the different mixture designs and materials  
156 used.

157 As illustrated in Fig. 1, two field experiments were conducted, each involving two WMA mixtures and one control  
 158 HMA. The first phase involved monitoring burner fuel consumption during asphalt mixture production to assess  
 159 energy savings. In the second phase, mixture performance was evaluated through AMPT testing, including dynamic  
 160 modulus, cyclic fatigue, and SSR tests. The resulting data were analyzed using FHWA's FlexMAT™ v2.2 to  
 161 evaluate material performance properties. Pavement performance, in terms of predicted percent damage and rutting,  
 162 was assessed using FlexPAVE™ v2.2.

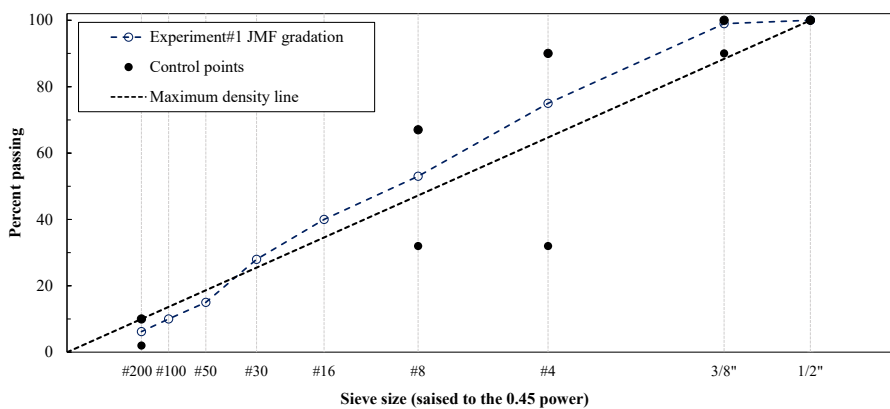


163  
 164 *Fig. 1. Test plan for Experiments 1 and 2*

165  
 166 **Experiment 1**

167 The first experiment was conducted at an asphalt plant in Montgomery, Alabama, as part of an overlay project on U.S.  
 168 Route 82 near Prattville. The facility operated a 2000 model Astec Double Barrel Green® drum mixer using recycled  
 169 No. 2 fuel oil. Three mixtures were produced: one control HMA and two WMA mixtures (WMA1 and WMA2),  
 170 containing different chemical additives.

171 All mixtures were produced using the same aggregate gradation and binder content. A PG 76-22 asphalt binder  
172 modified with 2.5% styrene-butadiene-styrene (SBS) polymer was used to meet ALDOT's traffic-based grade-  
173 bumping requirements (ALDOT 2022). The chemical WMA additives were terminally blended into the virgin binder  
174 at a dosage of 0.5% by weight, as recommended by the suppliers. WMA1 was a bio-based chemical additive with a  
175 relative density of 0.97 and viscosity of 127 cP at 25°C, while WMA2 was a bio-based chemical additive with a density  
176 of 0.98 g/mL, viscosity of 210 cP at 25 °C, and an open-cup flash point of 211°C. All mixtures included 20%  
177 Reclaimed Asphalt Pavement (RAP) and were designed as a fine-graded blend with a nominal maximum aggregate  
178 size (NMAS) of 9.5 mm (Fig. 2).



179

180 *Fig. 2. Aggregate gradation used in Experiment 1*

181

182 To minimize residual heat effects, each mixture was produced on a separate day. The control HMA was produced in  
183 September 2023 under an average ambient temperature of 30.2°C (86.4°F), followed by WMA1 the next day under  
184 similar conditions. WMA2 was produced in December 2023 due to a shipping delay, under significantly cooler  
185 ambient conditions (10.4°C or 50.7°F), around 20°C lower than the temperatures during the HMA and WMA1  
186 production.

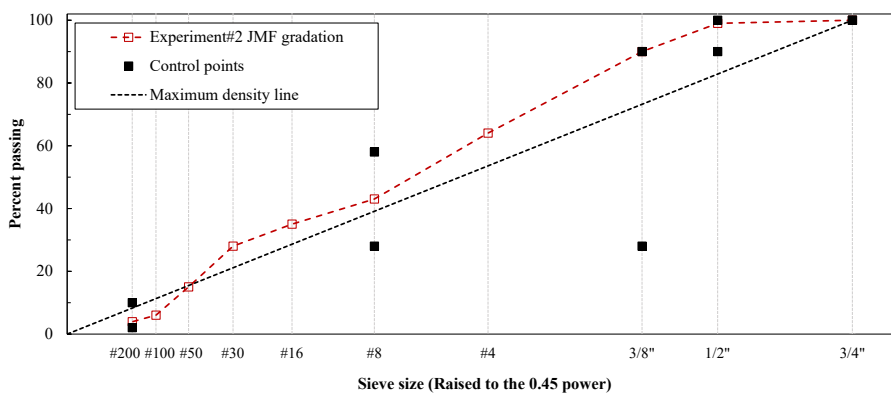
187 Target production temperatures were 160–166°C (320–330°F) for the HMA and 135–141°C (275–285°F) for the  
188 WMA mixtures. However, operational constraints—such as concurrent HMA production and mechanical issues—led  
189 to deviations. The actual average production temperatures were 162°C (323°F) for the HMA, 151°C (303°F) for  
190 WMA1, and 146°C (295°F) for WMA2, corresponding to temperature reductions of approximately 11°C (20°F) and  
191 16°C (28°F), respectively. The average aggregate moisture content was 2.0%, measured in accordance with AASHTO  
192 T255-22 (AASHTO 2022).

193 Burner fuel consumption was measured during production. Each plant run was allowed to stabilize at the target  
194 temperature before recording fuel usage and sampling to minimize the influence of residual heat. Loose mix samples  
195 were collected and transported to the laboratory, where Reheated Plant-Mixed Lab-Compacted (RH-PMLC)  
196 specimens were prepared following NAPA IS-145 guidelines (NAPA 2023). Compaction temperatures were  
197 approximately 135°C (275°F) for HMA and 116°C (240°F) for the WMA mixtures.

198

### 199 **Experiment 2**

200 Building on findings from the first experiment, a second field study was designed to evaluate the effects of more  
201 aggressive temperature reductions using the same WMA additive as in WMA1. This experiment was conducted at a  
202 different asphalt plant in Ariton, Alabama, equipped with a 2017 model CMI E3 drum mixer, four storage silos, and  
203 twin RAP cold feed systems. Recycled No. 2 fuel oil was again used as burner fuel. The experiment included one  
204 control HMA and one WMA mixture, with the latter produced and evaluated at two different target temperatures.  
205 All mixtures used the same aggregate gradation and binder content. A PG 67-22 binder was used for all mixtures,  
206 with the WMA binder terminally blended with 0.5% additive (by weight of virgin binder). The aggregate blend was  
207 fine-graded with an NMAS of 12.5 mm (Fig. 3).



208

209 *Fig. 3. Aggregate gradation used in Experiment 2*

210

211 Production was carried out in June 2024, under relatively stable ambient temperatures averaging approximately  
212 21°C (70°F). On the first day, the control HMA (HMA-325F) was produced at 163°C (325°F). On the second day,  
213 WMA production commenced after the plant stabilized at HMA conditions and was then progressively cooled to  
214 141°C (285°F) and 127°C (260°F). Fuel consumption and mix samples were recorded after thermal stabilization at

215 each temperature. RH-PMLC specimens were prepared by reheating the loose mixtures to their respective  
 216 compaction temperatures—approximately 140°C (285°F) for the HMA, and 124°C (255°F) and 113°C (235°F) for  
 217 the WMA samples—prior to immediate compaction, following NAPA IS-145 procedures (NAPA 2023).

218

### 219 **Mix Designs, Quality Control Data, and Production Variables**

220 Volumetric properties of the asphalt mixtures were evaluated based on contractor-reported Quality Control (QC)  
 221 data and compared against the Job Mix Formula (JMF) and Alabama Department of Transportation (ALDOT)  
 222 acceptance criteria. Volumetric specimens were compacted to 60 gyrations in accordance with ALDOT  
 223 specifications. Across both experiments, asphalt content closely matched JMF targets. Air voids and voids in  
 224 mineral aggregate (VMA) showed reductions—typically within one percent—but remained consistent among  
 225 mixtures within each experiment. These observations suggest that producing WMA at lower temperatures did not  
 226 significantly affect volumetric properties. Table 1 summarizes the QC data, JMF targets, and ALDOT criteria for all  
 227 mixtures.

228 *Table 1. Volumetric QC data compared to JMF and ALDOT criteria*

Experiment	Mixture	Asphalt Content (%)	Air Voids (%)	VMA (%)	VFA (%)	D/P <sub>be</sub>
Experiment 1	QC-HMA	5.50	3.96	16.0	75.3	1.22
	QC-WMA 1	5.53	4.18	16.6	74.8	1.07
	QC-WMA 2	5.44	3.70	15.4	75.9	1.15
	JMF	5.50	4.17	16.5	74.7	1.16
	JMF acceptance	≥ 5.5	4.0	≥ 15.5	N/A	0.6-1.4
Experiment 2	QC-HMA-325F	5.03	3.47	14.2	75.6	0.73
	QC-WMA-285F	5.09	3.36	14.2	76.3	0.85
	QC-WMA-260F	5.13	3.24	14.4	77.5	0.87
	JMF	5.10	4.4	15.1	73.5	0.77
	JMF acceptance	≥ 5.1	4.0	≥ 14.5	N/A	0.6-1.4

229

230 Table 2 presents production-related parameters, including production temperature (Based on one-time readings  
 231 recorded by the plant monitoring system), duration, total tonnage, and average production rate for each mixture.

232 *Table 2. Production temperature and tonnage data*

Experiment	Mixture	Temp	Duration (hr.)	Tonnage (t)	Production rate (t/hr)
Experiment 1	HMA	162°C (323°F)	6.5	945.3	145.4
	WMA1	151°C (303°F)	6.5	914.3	140.7
	WMA2	146°C (295°F)	3.5	522.0	149.1
Experiment 2	HMA-325F	163°C (325°F)	8.0	1881.3	235.2
	WMA-285F	141°C (285°F)	2.5	604.6	241.8
	WMA-260F	127°C (260°F)	4.0	1084.6	271.1

233

## 234 **Energy Consumption Data Collection and Analysis**

235 Both asphalt plants used recycled No. 2 fuel oil as the burner fuel, stored in on-site cylindrical tanks equipped with  
236 analog gauges. Fuel usage was recorded in gallons at 30-minute intervals during production, along with the  
237 corresponding tonnage of asphalt mixture produced. These data were used to calculate burner fuel consumption per  
238 short ton for each time interval using Eq. (1):

$$E_i = 140000 \times \frac{V_i}{M_i} \quad (1)$$

239 where:

240  $E_i$  = energy consumption during interval  $i$  (BTU/ton)

241  $V_i$  = volume of diesel used during interval  $i$  (gallon)

242  $M_i$  = tonnage of asphalt mixture produced during interval  $i$  (ton)

243 An energy intensity factor of 140,000 BTU per gallon of fuel was applied, consistent with U.S. Environmental  
244 Protection Agency data (Environmental Protection Agency 2024). The interval data were then aggregated to determine  
245 the average burner fuel consumption and associated variability for each mixture.

246 The interval data were then aggregated to determine the average energy consumption and its variability for each  
247 asphalt mixture. This method enabled a detailed evaluation of energy demand during production and facilitated direct  
248 comparisons of energy efficiency across different mixtures and production temperatures. It should be noted that energy  
249 consumption from hot oil heaters—used to heat the asphalt binder—was not included in this analysis.

250

## 251 **Laboratory Testing**

252 The performance properties of the asphalt mixtures were evaluated using the AMPT. Three tests were conducted:  
253 dynamic modulus ( $|E^*|$ ), cyclic fatigue, and SSR. The results from these tests served as required input parameters for  
254 subsequent pavement performance modeling of asphalt layers using the FlexPAVE™ program.

255

### 256 ***Dynamic Modulus Test***

257 The dynamic modulus ( $|E^*|$ ) test was conducted in accordance with AASHTO TP132-23 (AASHTO 2023) on small  
258 cylindrical specimens (38 mm diameter  $\times$  110 mm height), compacted to  $7.0 \pm 0.5\%$  air voids. Testing was performed

259 at three temperatures (4°C, 20°C, and 40°C) and three loading frequencies (10, 1, and 0.1 Hz) at each temperature. A  
260 sinusoidal compressive load was applied to induce axial peak-to-peak strains of 70–75 microstrain ( $\mu\epsilon$ ).  
261 The resulting data were used to construct  $|E^*|$  master curves using time–temperature superposition in accordance with  
262 AASHTO R84 (AASHTO 2021). The master curve was fitted using a sigmoidal model, as shown in Eq. (2):

$$\log|E^*| = \delta + \frac{(\text{Max} - \delta)}{1 + e^{\beta + \gamma \log f_r}} \quad (2)$$

263  
264 where,  $|E^*|$  = dynamic modulus, MPa;  $\delta, \beta, \gamma$  = fitting parameters,  $\text{Max}$  = the limiting minimum modulus, MPa; and  
265  $f_r$  = reduced frequency at the reference temperature, Hz.

266  
267 The reduced frequency was calculated using the Arrhenius equation, as shown in Eq. (3).

$$\log f_r = \log f + \frac{\Delta E_a}{19.14714} \left( \frac{1}{T} - \frac{1}{T_r} \right) \quad (3)$$

268  
269 where:  $f_r$  = Reduced frequency at the reference temperature, Hz;  $f$  = Reduced frequency at the test temperature, Hz;  
270  $T_r$  = Reference temperature, °K;  $T$  = Test temperature, °K;  $\Delta E_a$  = Activation energy (treated as a fitting parameter)

271  
272 The cracking resistance of the mixtures was evaluated using the Glover–Rowe parameter ( $G-R_m$ ). This evaluation  
273 followed the original formula developed for asphalt binders, but it used the ( $|E^*|$ ) test results. Lower  $G-R_m$  values  
274 indicate better cracking resistance.  $G-R_m$  was calculated based on Eq. (4) with a temperature and frequency  
275 combination of 20°C and 5 Hz (Oshone et al. 2019; Zhang et al. 2022).

$$G-R_m = \frac{|E^*|(\cos(\delta))^2}{\sin(\delta)} \quad (4)$$

276  
277 **Cyclic Fatigue Test**

278 Cyclic fatigue testing was conducted following AASHTO T411-24 (AASHTO 2024) using small specimens (38 mm  
279 diameter  $\times$  110 mm height) with  $7.0 \pm 0.5\%$  air voids and a 70 mm axial gauge length. Tests were performed at 21°C  
280 and 10 Hz and appropriate strain rates resulting in failure between 2,000 and 80,000 cycles. Strain levels employed

281 were in the range of 450–475  $\mu\epsilon$  for Experiment 1 and 375–450  $\mu\epsilon$  for Experiment 2, reflecting differences in mixture  
282 composition and, more notably, the effect of the polymer-modified binder in the first experiment.

283 FlexMAT™ v2.2 was used to analyze the laboratory test results. While the dynamic modulus data were analyzed and  
284 presented using the sigmoid and Arrhenius models, the cyclic fatigue analysis within FlexMAT™ v2.2 employed the  
285 2S2PID model and polynomial shift functions for dynamic modulus characterization. Key outputs included the  
286 damage characteristic curve (C–S curve), which plots pseudo stiffness versus damage, and the damage ratio ( $D^R$ )  
287 failure criterion, proposed by Wang and Richard Kim (2019) and Wang et al. (2022). Both were used in the  
288 FlexMAT™ v2.2 software (FHWA 2025) to calculate the cyclic fatigue index ( $S_{app}$ ), where higher values for both  
289 parameters indicate better fatigue performance.

290

### 291 ***Stress Sweep Rutting (SSR) Test***

292 SSR testing followed AASHTO TP134-22 (AASHTO 2022) using large cylindrical specimens (100 mm diameter  $\times$   
293 150 mm height), compacted to  $7.0 \pm 0.5\%$  air voids. Tests were performed at the low temperature (TL) of 26.2°C  
294 and high temperature (TH) of 51.2°C, determined based on the project locations. A constant confining pressure of  
295 69 kPa was maintained during the test.

296 Each test included three 200-cycle loading blocks at deviatoric stress levels of 483, 689, and 896 kPa for TL, and 689,  
297 483, and 896 kPa for TH. Each cycle consisted of a 0.4-second loading time, followed by rest periods of 1.6 seconds  
298 (TL) or 3.6 seconds (TH). Permanent deformation data were recorded and then analyzed using FlexMAT™ v2.2,  
299 which also calculated the Rutting Strain Index ( $RSI$ ). The  $RSI$  is calculated by dividing the permanent deformation of  
300 an asphalt layer by its thickness after 20 years of traffic loading, assuming 30 million 18-kip standard Equivalent  
301 Single Axle Load (ESAL). Lower  $RSI$  values indicate higher rutting resistance.

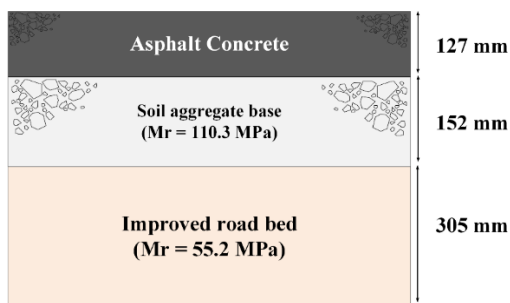
302

### 303 **Pavement Modeling using FlexPAVE™**

304 FlexPAVE™ v2.2 was used to predict the long-term pavement performance of a pavement structure utilizing the  
305 mixtures evaluated in the study. FlexPAVE™ is a mechanistic pavement analysis and design tool that accounts for  
306 moving traffic loads, temperature gradients, and asphalt aging over time (FHWA 2025; Wang et al. 2016). Fatigue

307 performance was predicted using the Simplified Viscoelastic Continuum Damage (S-VECD) model and input data  
308 from cyclic fatigue testing (Eslaminia and Guddati 2016), while rutting performance was estimated based on SSR test  
309 data and a permanent strain shift model (Ghanbari et al. 2022).

310 The modeled pavement structure consisted of three layers: a 127 mm (5 in.) asphalt concrete surface, a 152 mm (6 in.)  
311 unbound aggregate base, and a 305 mm (12 in.) improved subgrade (Fig. 4). The resilient modulus values for the base  
312 and subgrade were 110.3 MPa (16.0 ksi) and 55.2 MPa (8.0 ksi), respectively, following Alabama Department of  
313 Transportation (ALDOT) design recommendations. Material inputs for the asphalt layer were derived from AMPT  
314 testing and processed using FlexMAT™ v2.2. Site-specific climate and traffic conditions from the first project location  
315 were incorporated into the program. Additional inputs included a 20-year design life, an 18-kip axle load, 765 axles  
316 per day, 120 psi tire pressure, and a vehicle speed of 50 mph. Level III aging inputs—comprising RAP content,  
317 Recycled Binder Ratio (RBR), and high-temperature performance grades of both virgin and RAP-recovered binders—  
318 were used to simulate aging effects. Outputs included fatigue damage and rut depth progression over time. Thermal  
319 cracking was not evaluated, as FlexPAVE™ v2.2 does not currently support thermal cracking prediction.

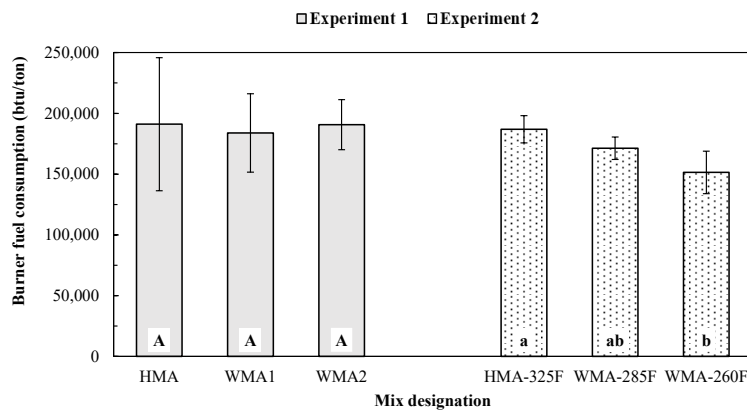


320  
321 *Fig. 4. Representative pavement Structure used for Modeling*  
322

323

## 324 RESULTS AND DISCUSSION

### 325 Burner Fuel Consumption Results



326

327 Fig. 5 presents the average burner fuel consumption for each mixture across both experiments, with error bars  
328 indicating  $\pm$  one standard deviation. Statistical comparisons were conducted using Tukey's Honestly Significant  
329 Difference (HSD) test in conjunction with one-way analysis of variance (ANOVA) at a 95% confidence level ( $\alpha =$   
330 0.05). Statistical groupings are denoted by letters above each bar—uppercase letters correspond to mixtures from  
331 Experiment 1, and lowercase letters correspond to those from Experiment 2. This convention is consistently used  
332 throughout the subsequent statistical comparisons in this section.

333 In Experiment 1, WMA1 exhibited slightly lower fuel consumption than the control HMA and WMA2; however, the  
334 differences were not statistically significant. This modest reduction in WMA1 can be attributed to its lower production  
335 temperature—approximately 11°C (20°F) below that of the control HMA—produced under similar ambient  
336 conditions. WMA2, produced at an even lower temperature (approximately 16°C or 28°F below the HMA), did not  
337 yield measurable energy savings, likely due to its production occurring on a much colder day, with ambient  
338 temperatures approximately 20°C (36°F) lower than those during HMA and WMA1 production, which may have  
339 offset potential fuel savings.

340 In Experiment 2, the effect of temperature reduction was more pronounced. Compared to the control HMA produced  
341 at 163°C (325°F), WMA mixtures produced at 141°C (285°F) and 127°C (260°F) reduced burner fuel consumption  
342 by approximately 8% and 19%, respectively. The reduction for the 127°C WMA was statistically significant. These  
343 findings confirm that substantial reductions in production temperature can yield meaningful energy savings without  
344 compromising production efficiency.

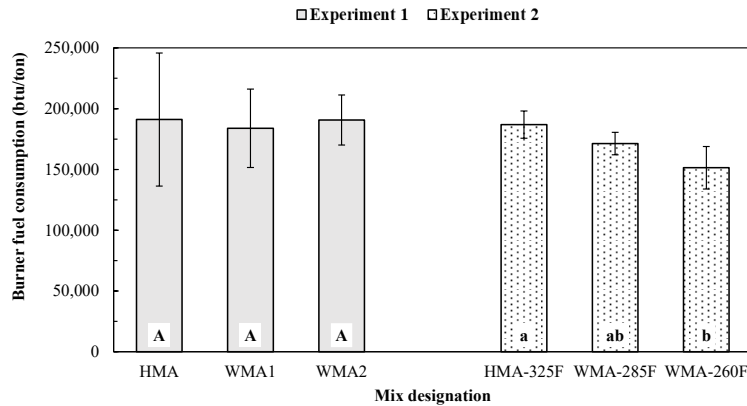


Fig. 5. Average Burner Fuel Consumption Results (Sadeghi et al. 2025)

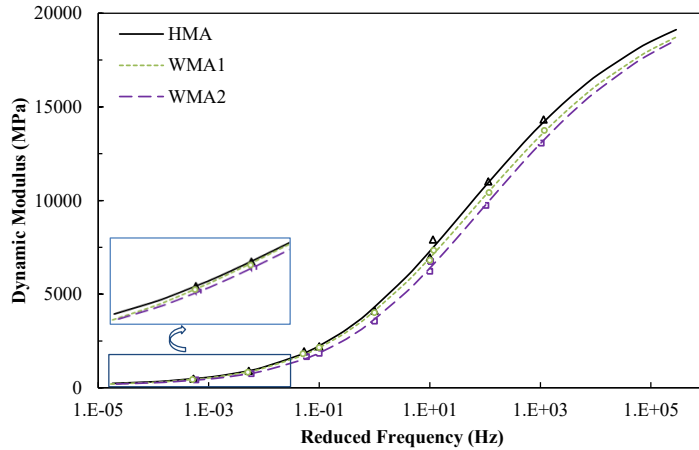
345  
346  
347

### 348 AMPT Performance Tests

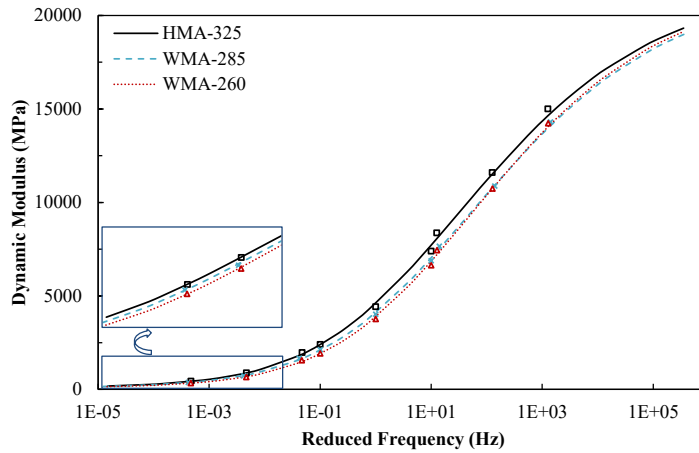
#### 349 *Dynamic Modulus ( $E^*$ ) and Phase Angle ( $\delta$ ) Results*

350 Dynamic modulus ( $|E^*|$ ) master curves are presented in Fig. 6. The plots show  $|E^*|$  on a numerical scale, with log-log  
351 insets illustrating behavior at the lowest reduced frequencies. The master curves were developed in accordance with  
352 AASHTO R84 (AASHTO 2021), independent of FlexMAT™ processing.

353 In Experiment 1 (Fig. 6a), both WMA mixtures exhibited lower  $|E^*|$  values across all temperatures and frequencies  
354 compared to the control HMA, with WMA2 showing the largest reduction. The lower stiffness observed at high and  
355 intermediate frequencies suggests enhanced flexibility and potentially improved resistance to thermal and fatigue  
356 cracking. However, the reduced  $|E^*|$  values at low frequencies—representative of higher pavement temperatures—  
357 suggest a decrease in rutting resistance. A similar trend was observed in Experiment 2 (Fig. 6b), where both WMA  
358 mixtures showed lower  $|E^*|$  values than the control HMA. The WMA mixture produced at 127°C (260°F) exhibited  
359 the lowest stiffness, suggesting that production temperature significantly influences mixture modulus.



a) Experiment 1 Results

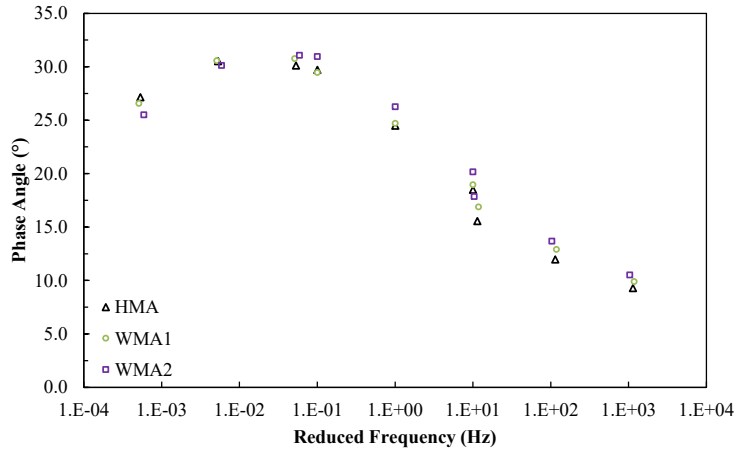


b) Experiment 2 Results

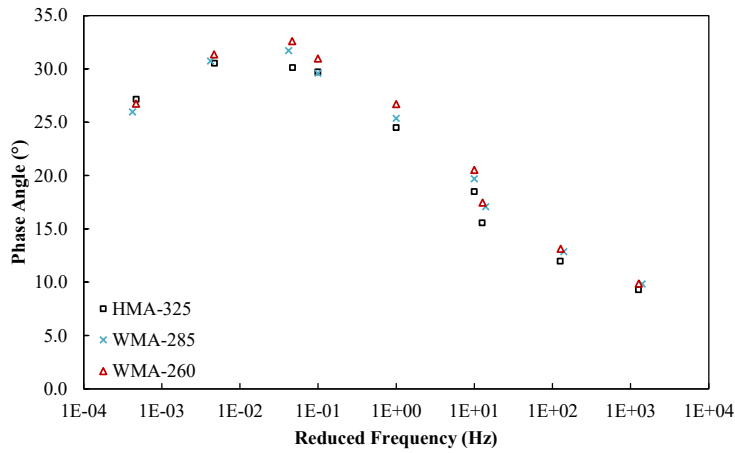
Fig. 6. Dynamic Modulus Master Curves

360  
361

362 Phase angle ( $\delta$ ) diagrams are shown in Fig. 7. In Experiment 1 (Fig. 7a), WMA mixtures exhibited slightly higher  $\delta$   
363 values at intermediate and high frequencies, indicating more viscous behavior. This suggests greater energy dissipation  
364 and enhanced resistance to intermediate- and low-temperature cracking. At low frequencies, WMA mixtures showed  
365 lower  $\delta$  values, reflecting more elastic behavior that may help reduce permanent deformation at high service  
366 temperatures. Similar behavior was observed in Experiment 2 (Fig. 7b).



a) Experiment 1 mixtures



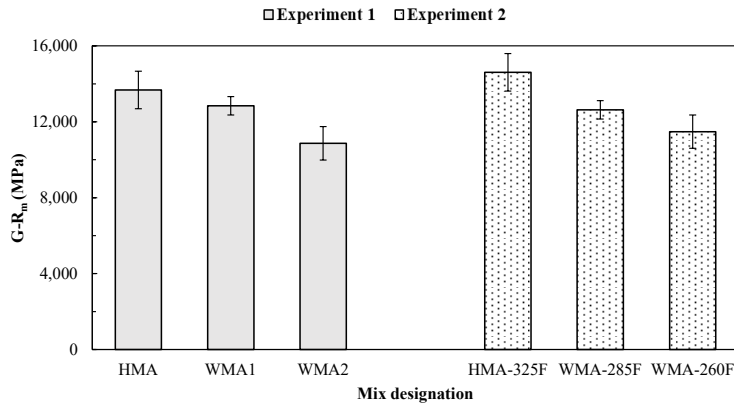
b) Experiment 2 mixtures

Fig. 7. Phase Angle Results

367  
368

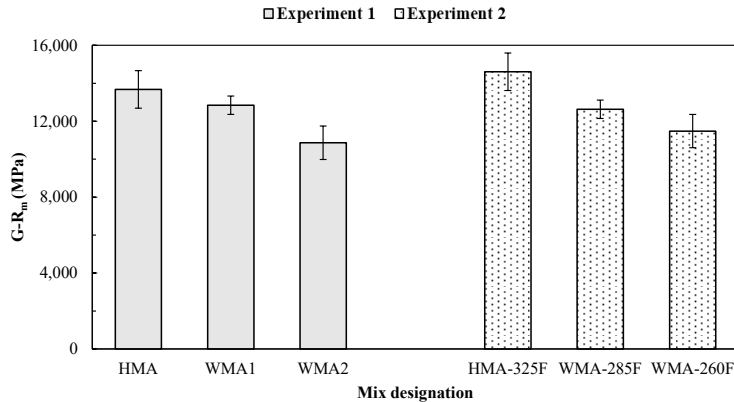
369 **Glomer Rowe Parameter**

370 The mixture Glover-Rowe parameter ( $G-R_m$ ), calculated from  $|E^*|$  and  $\delta$ , quantifies mixture stiffness and brittleness  
 371 to assess non-load-related cracking resistance. According to NCHRP Project 09-58, recommended thresholds for  $G-$   
 372  $R_m$  are 8,000 MPa for short-term aged and 19,000 MPa for long-term aged mixtures (Kim et al. 2021).



373

374 Fig. 8 presents the  $G-R_m$  results. Average values were obtained from fitted master curves based on three replicate  
375 specimens per mixture, with error bars representing the standard deviation of  $G-R_m$  calculated individually for each  
376 replicate. In Experiment 1, both WMA mixtures showed lower  $G-R_m$  values than the control HMA, with WMA2  
377 exhibiting the greatest reduction. Similar results were observed in Experiment 2, where the WMA produced at 127°C  
378 (260°F) had the lowest  $G-R_m$  value. These findings indicate that lowering production temperatures improved mixture  
379 flexibility and resistance to non-load-related (thermal or block) cracking.

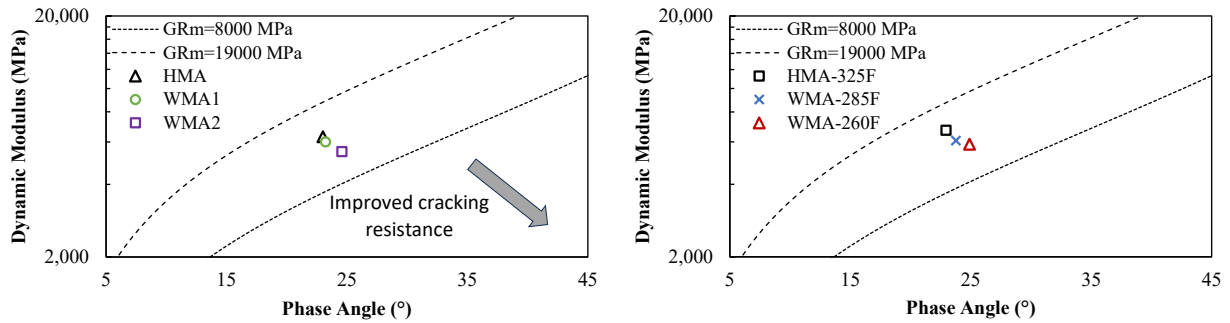


380

381 Fig. 8.  $G-R_m$  cracking susceptibility index results

382

383 Black space diagrams of  $|E^*|$  versus  $\delta$  on a logarithmic scale (Fig. 9) further support these observations. A shift toward  
384 the lower-right quadrant corresponds to lower  $G-R_m$  values and enhanced resistance to block or thermal cracking. In  
385 both experiments, WMA mixtures shifted consistently in this direction, with WMA2 and WMA-260F mixtures  
386 showing the most pronounced improvements.



a) Experiment 1 mixtures

b) Experiment 2 mixtures

387 Fig. 9. Mixture Black Space Diagrams

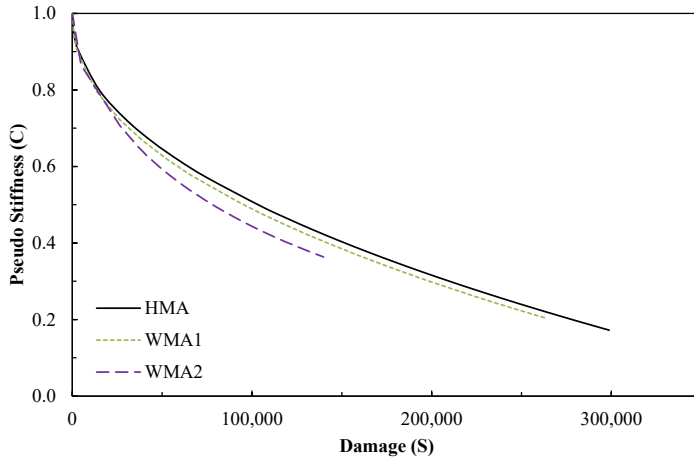
388  
389

### 390 **Cyclic Fatigue Test Results**

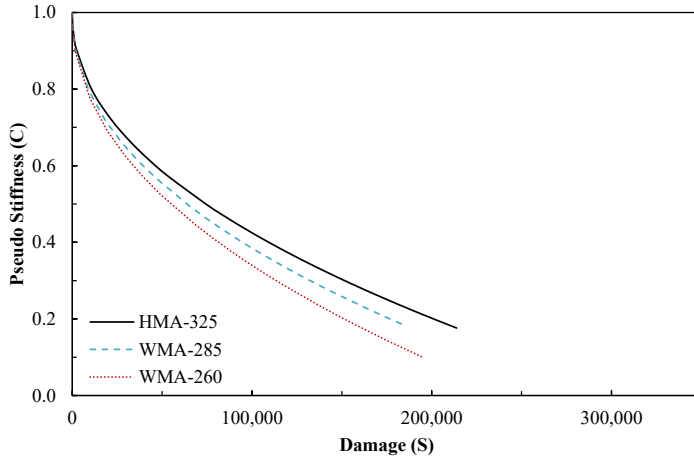
391 Cyclic fatigue performance was evaluated using FlexMAT™ v2.2, which applies the S-VECD model to generate  
392 damage characteristic (C-S) curves (Fig. 10). In these curves, pseudo-stiffness (C) decreases as damage (S)  
393 accumulates. In a fatigue damage tolerance (toughness) perspective, a steeper and shorter C-S curve indicates rapid  
394 stiffness degradation and faster fatigue damage progression (Kim et al. 2021).

395 WMA mixtures in both experiments exhibited shorter and flatter C-S curves than their HMA counterparts, suggesting  
396 that while WMA mixtures absorbed strain energy effectively at early stages, damage accumulated more rapidly after  
397 initiation. Across the full range of S values, the C-S curves for control HMA mixtures consistently lie above those of  
398 the WMA mixtures, suggesting higher stiffness and slower damage progression (Wang et al. 2022). A stiffer mix  
399 under the same load amplitude would experience lower strain, which generally translates to longer fatigue life (Wang  
400 et al. 2022).

401



a) Experiment 1 mixtures

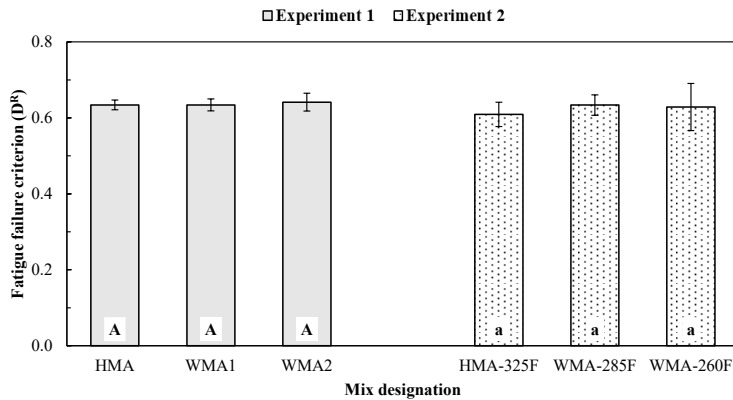


b) Experiment 2 mixtures

Fig. 10. Damage Characteristics Curve (C-S curve) Results

402  
403

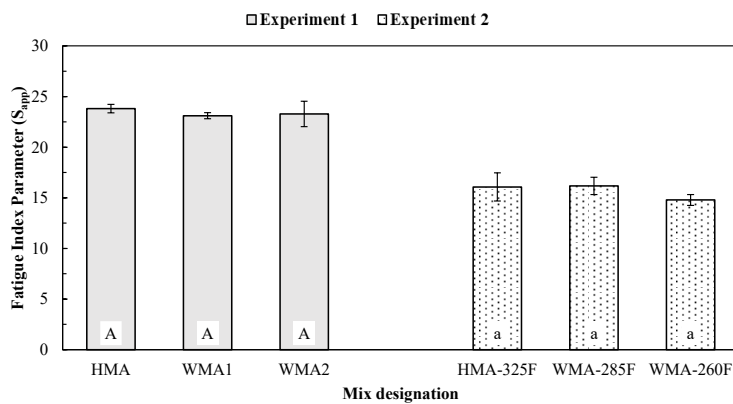
404 FlexMAT™ also calculates two key fatigue parameters: the  $D^R$  failure criterion and the apparent damage capacity  
405 ( $S_{app}$ ) (Fig. 11 and 12).  $D^R$  represents fatigue damage tolerance (toughness), whereas the  $S_{app}$  parameter accounts for  
406 the combined effects of stiffness and toughness. Across both experiments,  $D^R$  and  $S_{app}$  values were similar between  
407 WMA and HMA mixtures, indicating comparable overall fatigue performance. In Experiment 2, consistent  $D^R$  and  
408  $S_{app}$  values across all mixtures confirmed that further reductions in production temperature did not impact fatigue  
409 resistance.



410

411 Fig. 11. Fatigue Failure Criterion ( $D^R$ ) Results

412



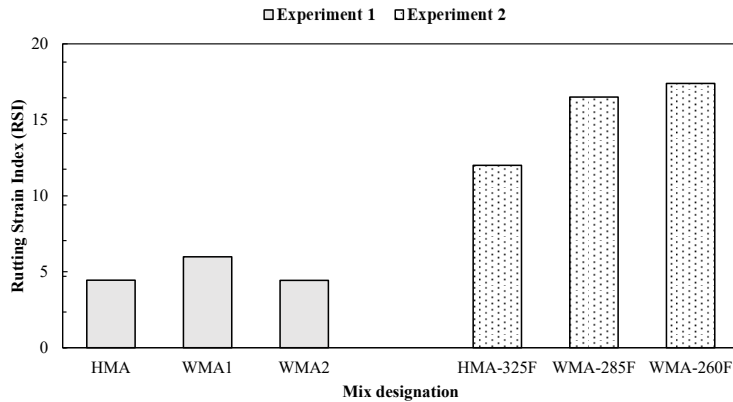
413

414 Fig. 12. Fatigue Index Parameter ( $S_{app}$ ) Results

415

### 416 **Stress Sweep Rutting Results**

417 Fig. 13 presents the *RSI* results, calculated from the SSR test to estimate the average permanent strain accumulated  
418 over 20 years of traffic loading (assuming 30 million ESALs). In both experiments, WMA mixtures exhibited higher  
419 RSI values than the control HMA, indicating increased susceptibility to rutting. In Experiment 1, WMA1 had the  
420 highest RSI, underscoring the influence of additive type. In Experiment 2, RSI values increased with decreasing  
421 production temperature, with the WMA produced at 127°C (260°F) showing the highest rutting potential. These results  
422 are consistent with the dynamic modulus findings, which showed lower stiffness for WMA mixtures. The overall  
423 trends suggest that while lower production temperatures improve flexibility and cracking resistance, they may also  
424 reduce rutting resistance—particularly at the lowest production temperatures.



425

426 *Fig. 13. RSI Rutting Index Results*

427

### 428 **5.5 Performance Modeling Using FlexPAVE™**

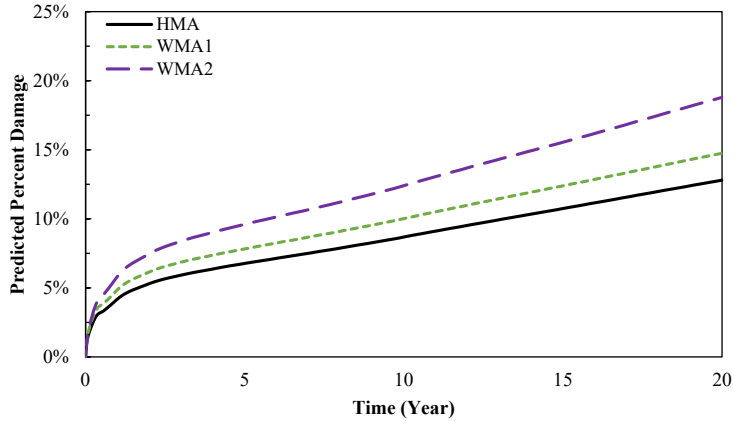
#### 429 *Analysis of Damage Evolution*

430 FlexPAVE™ modeling was conducted using a three-layer pavement structure, with asphalt surface layer properties  
431 derived from AMPT test results. Predicted fatigue damage evolution over a 20-year design life is shown in Fig. 14.

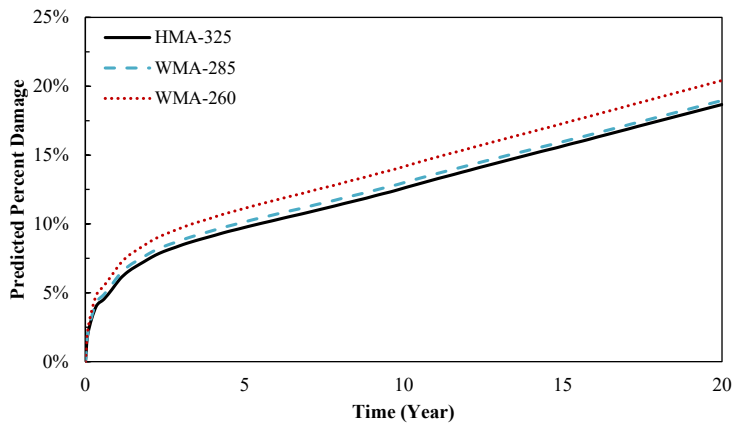
432 In Experiment 1 (Fig. 14a), both WMA mixtures exhibited higher cumulative predicted fatigue damage than the  
433 control HMA. After 20 years, WMA1 exhibited a 1.9% increase in damage, while WMA2 showed a 6.0% increase.  
434 These results suggest that WMA1 performed comparably to the control HMA in predicted fatigue resistance, despite  
435 the higher damage predicted.

436 In Experiment 2 (Fig. 14b), reducing the production temperature by 22°C (40°F) for WMA-285F resulted in only a  
437 0.3% increase in fatigue damage compared to the control HMA. A 36°C (65°F) temperature reduction for WMA-260F  
438 led to a 1.8% increase in predicted fatigue damage. These modest increases indicate that significant temperature  
439 reductions can be achieved without substantially impacting long-term predicted fatigue performance when using  
440 chemical WMA additives.

441 It is essential to note that, although the same additive (WMA1) was used in both experiments, a direct comparison  
442 across experiments is not appropriate due to differences in materials, mix designs, and reheating and compaction  
443 temperatures. Therefore, predicted performance trends should be interpreted within each experiment independently.



a) Experiment 1 mixtures



b) Experiment 2 mixtures

444 Fig. 14. Predicted Percent Damage Using FHWA's FlexPAVETM Modeling

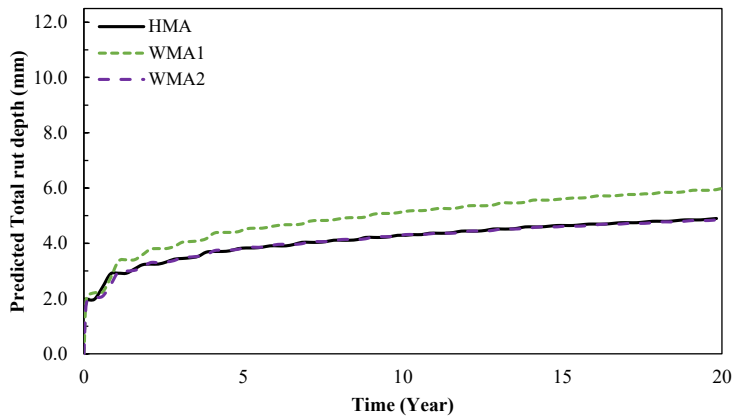
445

446 *Rutting Prediction*

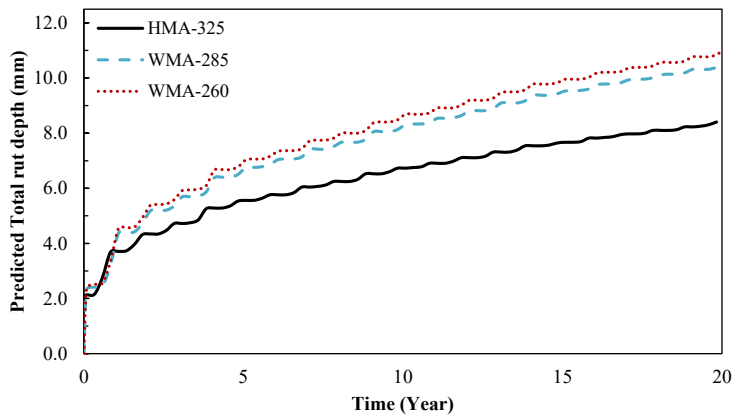
447 Predicted total rut depths are presented in Fig. 15. In Experiment 1 (Fig. 15a), WMA1 exhibited the highest predicted  
448 rut depth (6.0 mm), while WMA2 and the control HMA showed similar values (approximately 4.9 mm). These results  
449 align with the laboratory RSI data, indicating that WMA2 maintained rutting resistance comparable to that of the  
450 control, despite its lower stiffness.

451 In Experiment 2 (Fig. 15b), predicted rut depths were higher overall, primarily due to the use of an unmodified PG  
452 67-22 binder rather than the polymer-modified PG 76-22 used in Experiment 1. WMA mixtures exhibited greater  
453 rutting than the control HMA, with WMA-285F and WMA-260F showing 2.1 mm and 2.6 mm higher rut depths,

454 respectively. The marginal difference between these two WMA mixtures suggests that additional temperature  
455 reductions beyond 141°C (285°F) had a limited effect on rutting performance.



a) Experiment 1 mixtures



b) Experiment 2 mixtures

456 Fig. 15. Predicted Total Rut Depth Using FHWA's FlexPave™ Modeling  
457

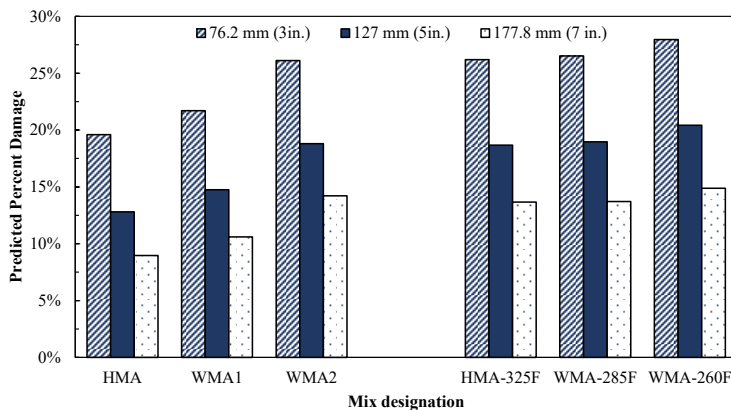
458 Overall, the FlexPAVE™ modeling results indicated that WMA mixtures can achieve long-term fatigue  
459 performance comparable to conventional HMAs, with a modest increase in predicted rutting susceptibility. Because  
460 FlexPAVE™ v2.2 does not currently model thermal cracking, future inclusion of this feature would likely further  
461 highlight the benefits of WMA mixtures for improving low-temperature performance.

462 *Effect of Layer Thickness*

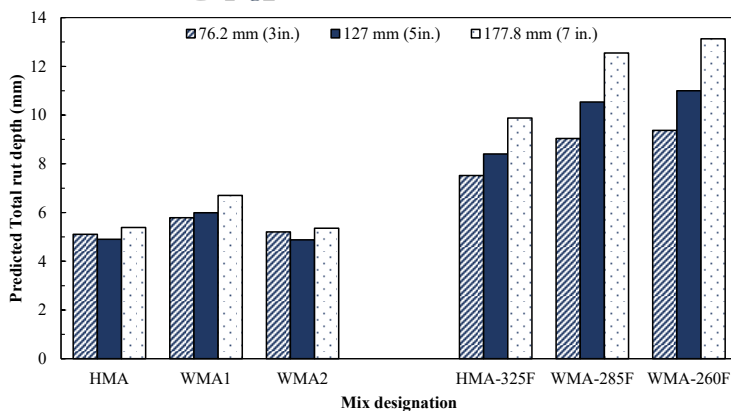
463 The influence of asphalt layer thickness on pavement performance was also evaluated using FlexPAVE™. Three  
464 surface thickness scenarios were modeled: a standard 127 mm (5 in.) layer, a thinner 76.2 mm (3 in.) layer, and a  
465 thicker 177.8 mm (7 in.) layer.

466 As shown in Fig. 16, increasing the asphalt layer thickness consistently reduced predicted fatigue damage for all  
467 mixtures, which aligns with the expected reduction in tensile strain at the bottom of the asphalt layer. However, rutting  
468 behavior exhibited different trends between experiments. In Experiment 1, variations in layer thickness resulted in  
469 only minor changes in predicted rutting, with no discernible trend. In Experiment 2, predicted rutting increased slightly  
470 with thicker asphalt layers, likely due to the softer binder and higher internal strain levels in these mixtures.

471 Importantly, variations in asphalt thickness did not alter the relative performance ranking between WMA and HMA  
472 mixtures. This consistency reinforces the robustness of the findings and indicates that WMA mixtures can be reliably  
473 implemented across typical pavement thickness ranges without impacting performance.



a) Predicted Percent Damage



b) Predicted Total Rut Depth

Fig. 16. Predicted Percent Damage and Total Rut Depth for Different Asphalt Layer Thicknesses

474  
475

## 476 CONCLUSIONS

477 This study evaluated the effects of reducing asphalt production temperatures using chemical WMA additives on burner  
478 fuel consumption, mixture performance properties, and predicted pavement performance. Two field experiments were  
479 conducted using approved mix designs. Experiment 1 compared two chemical WMA additives with a conventional  
480 HMA control, while Experiment 2 focused on further reducing production temperatures using one of the WMA  
481 additives used in the first experiment. Key findings are summarized as follows:

- 482 • **Energy Consumption:** In Experiment 1, moderate reductions in production temperature did not yield  
483 measurable burner fuel savings. In Experiment 2, reducing production temperatures by 22°C (40°F) and 36°C  
484 (65°F) resulted in approximately 8% and 19% decreases in burner fuel usage, respectively, compared to the  
485 control HMA.
- 486 • **Cracking Performance:** AMPT testing showed that WMA mixtures produced at lower temperatures  
487 exhibited lower Glover–Rowe ( $G-R_m$ ) values, indicating improved non-load-related cracking resistance.  
488 Fatigue parameters, including the  $D^R$  and the  $S_{app}$ , remained comparable between WMA and HMA mixtures,  
489 suggesting that reducing production temperatures did not affect fatigue performance.
- 490 • **Rutting Performance:** SSR test results indicated that WMA mixtures were more susceptible to permanent  
491 deformation than the control HMA, especially at the lowest production temperature. These findings  
492 underscore the importance of evaluating rutting potential when implementing significant reductions in  
493 production temperature.
- 494 • **Predicted Performance:** FlexPAVE™ modeling showed that WMA mixtures generally achieved similar  
495 fatigue performance to conventional HMA, with only modest increases in predicted rutting. The results  
496 suggest that temperature reductions are feasible without affecting overall pavement durability.

497 Overall, this research demonstrates that WMA technologies can substantially reduce burner fuel consumption and  
498 associated greenhouse gas emissions while maintaining acceptable performance. With appropriate mix design  
499 adjustments, WMA can offer a viable and sustainable solution for reducing asphalt production temperatures and  
500 enhancing energy efficiency in pavement construction.

501

502 **DATA AVAILABILITY STATEMENT:**

503 Some or all data, models, or code that support the findings of this study are available from the corresponding author  
504 upon reasonable request.

505

506 **ACKNOWLEDGEMENTS:**

507 The research project is funded through the Climate Challenge grant provided by the Federal Highway  
508 Administration to the Alabama Department of Transportation (ALDOT).

509

510 **REFERENCES**

- 511 AASHTO (2021). "AASHTO R84-17 (2021): Standard Practice for Developing Dynamic Modulus  
512 Master Curves for Asphalt Mixtures Using the Asphalt Mixture Performance Tester  
513 (AMPT)." *ASTM Compass*.
- 514 AASHTO (2022). "AASHTO T255-22 Standard Method of Test for Total Evaporable Moisture Content  
515 of Aggregate by Drying."
- 516 AASHTO (2022). "AASHTO TP134-22 Standard Method of Test for Stress Sweep Rutting (SSR) Test  
517 Using Asphalt Mixture Performance Tester (AMPT)."
- 518 AASHTO (2023). "AASHTO T132-23 Standard Method of Test for Determining the Dynamic Modulus  
519 for Asphalt Mixtures Using Small Specimens in the Asphalt Mixture Performance Tester  
520 (AMPT)."
- 521 AASHTO (2024). "AASHTO T411-24 Standard Method of Test for Determining the Damage  
522 Characteristic Curve and Failure Criterion Using Small Specimens in the Asphalt Mixture  
523 Performance Tester (AMPT) Cyclic Fatigue Test."
- 524 Akentuna, M., Mohammad, L. N., Boateng, K. A., and Cooper Jr, S. (2022). "Warm Mix Asphalt  
525 demonstration projects in Louisiana: Case study of five to eight years of field performance."  
526 *Transportation Research Record*, 2676(9), 148-158.
- 527 ALDOT (2022). "Standard Specifications for Highway Construction, Section 424  
528 (d)."<https://www.dot.state.al.us/publications/Construction/Specifications.html>.
- 529 Almeida-Costa, A., and Benta, A. (2016). "Economic and environmental impact study of warm mix  
530 asphalt compared to hot mix asphalt." *Journal of Cleaner Production*, 112, 2308-2317.
- 531 Bairgi, B. K., Rahman, A. A., Tarefder, R. A., and Larrain, M. M. M. (2020). "Comprehensive evaluation  
532 of rutting of warm-mix asphalt utilizing long-term pavement performance specific pavement  
533 studies." *Transportation Research Record*, 2674(7), 272-283.
- 534 Bairgi, B. K., Tarefder, R. A., Syed, I., Mendez, M. M., Ahmed, M., Mannan, U. A., and Rahman, M. T.  
535 "Assessment of Rutting Behavior of Warm-Mix Asphalt (WMA) with Chemical WMA Additives  
536 towards Laboratory and Field Investigation." *Proc., International Conference on Transportation  
537 and Development 2018*, American Society of Civil Engineers Reston, VA, 264-272.
- 538 Capitão, S., Picado-Santos, L., and Martinho, F. (2012). "Pavement engineering materials: Review on the  
539 use of warm-mix asphalt." *Construction and Building Materials*, 36, 1016-1024.

- 540 Cheraghian, G., Falchetto, A. C., You, Z., Chen, S., Kim, Y. S., Westerhoff, J., Moon, K. H., and  
541 Wistuba, M. P. (2020). "Warm mix asphalt technology: An up to date review." *Journal of*  
542 *Cleaner Production*, 268, 122128.
- 543 Croteau, J.-M., and Tessier, B. "Warm mix asphalt paving technologies: a road builder's perspective."  
544 *Proc., Annual Conference of the Transportation Association of Canada, Toronto, Citeseer.*
- 545 Dao, D. V., Nguyen, N.-L., Nguyen, M. H., Ly, H.-B., and Truong, V. Q. (2022). "Evaluation of cracking  
546 resistance of warm mix asphalt incorporating high reclaimed asphalt pavement content."  
547 *Proceedings of the Institution of Mechanical Engineers, Part L: Journal of Materials: Design and*  
548 *Applications*, 236(12), 2550-2560.
- 549 Environmental Protection Agency (2024). "Managing Used Oil: Answers to Frequent Questions for  
550 Businesses." <[https://www.epa.gov/hw/managing-used-oil-answers-frequent-questions-](https://www.epa.gov/hw/managing-used-oil-answers-frequent-questions-businesses)  
551 [businesses](https://www.epa.gov/hw/managing-used-oil-answers-frequent-questions-businesses)>. (July 31, 2024).
- 552 Epps, J. A. (2019). "Innovative asphalt pavement technology: paving the way for the world's roadways."  
553 *Transportation Research Record*, 2673(1), 1-16.
- 554 Eslaminia, M., and Guddati, M. N. (2016). "Fourier-finite element analysis of pavements under moving  
555 vehicular loading." *International Journal of Pavement Engineering*, 17(7), 602-614.
- 556 Fakhri, M., Ghanizadeh, A. R., and Omrani, H. (2013). "Comparison of fatigue resistance of HMA and  
557 WMA mixtures modified by SBS." *Procedia-Social and Behavioral Sciences*, 104, 168-177.
- 558 FHWA (2025). "Federal Highway Administration Asphalt Material Analysis Tools ",  
559 <<https://highways.dot.gov/turner-fairbank-highway-research-center/software/flexmat>>. (June 19,  
560 2025).
- 561 Garcia Cucalon, L., Kassem, E., Little, D. N., and Masad, E. (2017). "Fundamental evaluation of moisture  
562 damage in warm-mix asphalts." *Road Materials and Pavement Design*, 18(sup1), 258-283.
- 563 Ghanbari, A., Underwood, B. S., and Kim, Y. R. (2022). "Development of a rutting index parameter  
564 based on the stress sweep rutting test and permanent deformation shift model." *International*  
565 *Journal of Pavement Engineering*, 23(2), 387-399.
- 566 Kim, Y. R., Castorena, C., Saleh, N. F., Braswell, E., Elwardany, M., and Rad, F. Y. (2021). *Long-term*  
567 *aging of asphalt mixtures for performance testing and prediction: Phase III results.*
- 568 McCarthy, L., and Daniel, J. (2018). "Increasing WMA implementation by leveraging the state-of-the  
569 knowledge." *Final Report, NCHRP Project, 20, Task 01.*
- 570 NAPA (2023). "NAPA IS-145 Guide on Asphalt Mixture Specimen Fabrication for BMD Performance  
571 Testing."
- 572 NAPA (2024). "NAPA Quarterly: Pioneering Sustainable Pavements, Volume 29, Number 2, Summer  
573 2024."
- 574 Oshone, M., Sias, J. E., Dave, E. V., Epps Martin, A., Kaseer, F., and Rahbar-Rastegar, R. (2019).  
575 "Exploring master curve parameters to distinguish between mixture variables." *Road Materials*  
576 *and Pavement Design*, 20(sup2), S812-S826.
- 577 Padula, F. R., Nicodemos, S., Mendes, J. C., Willis, R., and Taylor, A. (2019). "Evaluation of fatigue  
578 performance of high RAP-WMA mixtures." *International Journal of Pavement Research and*  
579 *Technology*, 12, 430-434.
- 580 Rahman, M. A., Zaman, M., Ali, S. A., Ghabchi, R., and Ghos, S. (2022). "Evaluation of mix design  
581 volumetrics and cracking potential of foamed Warm Mix Asphalt (WMA) containing Reclaimed  
582 Asphalt Pavement (RAP)." *International Journal of Pavement Engineering*, 23(10), 3454-3466.
- 583 Rubio, M. C., Martínez, G., Baena, L., and Moreno, F. (2012). "Warm mix asphalt: an overview." *Journal*  
584 *of cleaner production*, 24, 76-84.
- 585 Sadeghi, M., Bairgi, B. K., Hartzog, Z., Gatiganti, S. C., Vangala, R. R., Jafarmilajerdi, A., Dylla, H.,  
586 Tran, N., and Bowers, B. (2025). "Effects of Reducing Asphalt Production Temperatures Using  
587 Warm Mix Technologies on Burner Fuel Consumption and Mixture Performance Properties."  
588 *Transportation Research Record*, 03611981251352508.
- 589 Sadeghi, M., and Sabouri, M. (2025). "Cracking indices and effects of synthetic fibres on the mechanical  
590 properties of cold recycled asphalt mixtures." *Road Materials and Pavement Design*, 1-24.

- 591 Spadoni, S., Ingrassia, L. P., Mariani, E., Cardone, F., and Canestrari, F. (2022). "Long-term performance  
592 assessment of a warm recycled motorway pavement." *Case Studies in Construction Materials*, 17,  
593 e01451.
- 594 Sukhija, M., Saboo, N., and Pani, A. (2022). "Economic and environmental aspects of warm mix asphalt  
595 mixtures: A comparative analysis." *Transportation Research Part D: Transport and*  
596 *Environment*, 109, 103355.
- 597 Wang, Y., Norouzi, A., and Kim, Y. R. (2016). "Comparison of fatigue cracking performance of asphalt  
598 pavements predicted by pavement ME and LVECD programs." *Transportation Research Record*,  
599 2590(1), 44-55.
- 600 Wang, Y., and Richard Kim, Y. (2019). "Development of a pseudo strain energy-based fatigue failure  
601 criterion for asphalt mixtures." *International Journal of Pavement Engineering*, 20(10), 1182-  
602 1192.
- 603 Wang, Y. D., Underwood, B. S., and Kim, Y. R. (2022). "Development of a fatigue index parameter,  
604 Sapp, for asphalt mixes using viscoelastic continuum damage theory." *International Journal of*  
605 *Pavement Engineering*, 23(2), 438-452.
- 606 Wen, H., Wu, S., Mohammad, L. N., Zhang, W., Shen, S., and Faheem, A. (2016). "Long-term field  
607 rutting and moisture susceptibility performance of warm-mix asphalt pavement." *Transportation*  
608 *Research Record*, 2575(1), 103-112.
- 609 West, R., Rodezno, C., Julian, G., Prowell, B., Frank, B., Osborn, L. V., and Kriech, T. (2014). *Field*  
610 *performance of warm mix asphalt technologies*.
- 611 West, R., Rodezno, C., Leiva, F., and Yin, F. (2018). "Development of a framework for balanced mix  
612 design." *Project NCHRP*, 20-07.
- 613 Williams, B. A., Willis, J. R., and Shacat, J. (2024). "Asphalt Pavement Industry Survey on Recycled  
614 Materials and Warm-Mix Asphalt Usage: 2022."
- 615 Yin, F., West, R., Powell, B., and DuBois, C. (2023). "Short-term performance characterization and  
616 fatigue damage prediction of asphalt mixtures containing polymer-modified binders and recycled  
617 plastics." *Transportation Research Record*, 03611981221143119.
- 618 Zaremotekhasas, F., Sadek, H., Hassan, M., and Berryman, C. (2022). "Impact of warm-mix asphalt  
619 technologies and high reclaimed asphalt pavement content on the performance of alternative  
620 asphalt mixtures." *Construction and Building Materials*, 319, 126035.
- 621 Zaumanis, M. (2014). "Warm mix asphalt." *Climate change, energy, sustainability and pavements*,  
622 Springer, 309-334.
- 623 Zhang, R., Sias, J. E., and Dave, E. V. (2022). "Evaluation of the cracking and aging susceptibility of  
624 asphalt mixtures using viscoelastic properties and master curve parameters." *Journal of traffic*  
625 *and transportation engineering (English Edition)*, 9(1), 106-119.

626